2010 IEEE International Conference on Robotics and Automation
Anchorage Convention District
May 3-8, 2010, Anchorage, Alaska, USA

Design and Experimental Verification of a Constrained Finite Time Optimal Control Scheme for the Attitude Control of a Quadrotor Helicopter Subject to Wind Gusts

Kostas Alexis, George Nikolakopoulos and Anthony Tzes*

Abstract— **In this paper the design and the experimental verification of a Constrained Finite Time Optimal (CFTO) control scheme for the attitude control of an Unmanned Quadrotor Helicopter (UqH) subject to wind gusts is being presented. In the proposed design the UqH has been modeled by a set of Piecewise Affine (PWA) linear equations while the wind gusts effects are embedded in the system model description as the affine terms. In this approach the switching among the PWA model descriptions are ruled by the rate of the rotation angles. In the design of the stabilizing CFTO–controller both the magnitude of external disturbances (worst case applied wind gust), and the mechanical constraints of the UqH such as maximum thrust in the rotors and UqH's angles rate are taken under consideration in order to design an off–line controller that could rapidly be applied to a UqH in a form of a look–up table. The proposed control scheme is applied in experimental studies and multiple test–cases are presented that prove the efficiency of the proposed scheme.**

I. INTRODUCTION

Over the last years, the area of Unmanned Aerial Vehicles (UAVs), and specially the quadrotor helicopters [1, 2] are gaining an increasing scientific attention. These helicopters are a special member of the rotorcraft family and excluding its high energy consumption, the quadrotor has outstanding capabilities on the issues of maneuverability, survivability, simplicity of mechanics and increased payload [3].

The UqH's hovering ability makes possible an extended area of applications for which fixed wing aircrafts are not suitable, due to their flight characteristics. Examples include forest fire surveillance [4], inspection of buildings and bridges [5], wildfire monitoring, law enforcement [6], and military applications. During all these missions precise, trajectory tracking with robustness with respect to disturbances is required.

From another point of view these UqHs, when flying in low–altitudes, which is the most typical characteristic for their flight, are prone to sudden wind–gusts. In most of the cases the windgusts density and direction can be detrimental in the performance and the overall stability of the UqH (e.g. path declination, crash). Handling of these sudden and unpredicted wind disturbances on the UqHs flight, requires that the atmospheric turbulence is modeled appropriately as random disturbances affecting the nominal system's description.

The authors are with Faculty of Electrical and Computer Engineering, University of Patras, 26500 Rio, Achaia, Greece.
*Corresponding Author's coordinates:tzes@ece.upatras.gr

The development and experimental verification of constrained finite time optimal controllers that could take under consideration: (a) the disturbances from the environment, and b) the physical and mechanical constraints of the system is the main contribution of this article. In the proposed control scheme, these factors that degrade the system's performance are embedded in the system model during the modeling phase for the control problem synthesis.

Until now in the relevant literature of UqHs, the problem of control design has been addressed using several methods such as the development of PID and LQR controllers in [7, 8], a Sliding Mode controller in [9, 10], and Nonlinear Dynamic Inversion and Backstepping in [11]. However, the main focus of this article is to: a) present an optimal constrained finite time control design approach, b) to apply the proposed control scheme in experimental results, and c) evaluate the overall experimental performance under various wind gusts and modeling approaches using PWA systems. To the authors' best knowledge this is the first time that a CFTO–control scheme is designed and experimentally applied for attitude control of a UqH under the effect of atmospheric turbulence.

This paper is structured as follows. In Section II, the modeling approach for the UqH is presented while in Section III the design and the development of the CFTO–control scheme is analyzed. In Section IV, the experimental results that prove the efficacy of the proposed scheme are presented, followed by conclusions.

II. QUADROTOR HELICOPTER MODELING

The modeling of the Unmanned quadrotor Helicopter shown in Figure 1, assumes that the structure is rigid and symmetrical, the center of gravity and the body fixed frame origin coincide, the propellers are rigid and the thrust and drag forces are proportional to the square of propeller's speed.

The UqH's nonlinear dynamics [11] is characterized by a set of twelve high non–linear state equations in the form:

$$\dot{\mathbf{X}} = f(\mathbf{X}, \mathbf{U}) + \mathbf{W} \tag{1}$$

with f a non–linear function, $\mathbf{W}$ corresponds to the additive effects of the environmental (wind) disturbances, $\mathbf{X}$ the state vector, and $\mathbf{U}$ the input vector, where:

$$\mathbf{X} = [\phi \;\; \dot{\phi} \;\; \theta \;\; \dot{\theta} \;\; \psi \;\; \dot{\psi} \;\; z \;\; \dot{z} \;\; x \;\; \dot{x} \;\; y \;\; \dot{y}] \tag{2}$$

$$\mathbf{U} = [U_1 \;\; U_2 \;\; U_3 \;\; U_4 \;\; \Omega_r] \; . \tag{3}$$

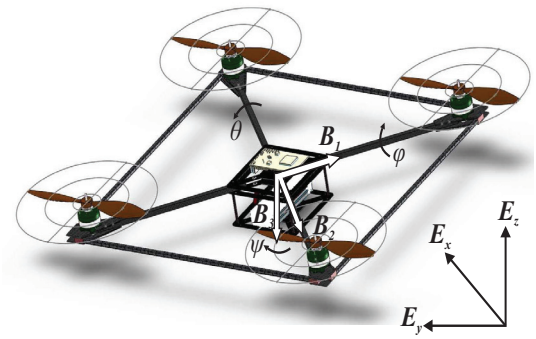

Fig. 1. Quadrotor helicopter configuration frame system

The control inputs in (1) are produced by the following combinations of the angular speeds of the four UqH's rotors as:

$$\begin{aligned} U_1 &= b(\Omega_1^2+\Omega_2^2+\Omega_3^2+\Omega_4^2) \\ U_2 &= b(-\Omega_2^2+\Omega_4^2) \\ U_3 &= b(\Omega_1^2-\Omega_3^2) \\ U_4 &= d(-\Omega_1^2+\Omega_3^2-\Omega_3^2+\Omega_4^2) \\ \Omega_r &= -\Omega_1+\Omega_2-\Omega_3+\Omega_4 \end{aligned}$$

where b is the thrust coefficient, and d is the drag coefficient, while the input U_1 is related with the total thrust and the inputs U_2, U_3, U_4 are related with the rotations of the quadrotor and Ω_r is the overall residual angular velocity of the motors. Under a small angle approximation and other assumptions and further simplifications that can be found in [11, 12] the system can be decoupled in two independent but connected subsystems. The first one is related to the linear translations and the second one deals with the angular rotations. The attitude equations correspond to the first six equations of the nonlinear ODEs in (1); small perturbations around the operating points $\mathbf{x}^{\circ,\mathbf{j}} = \left[0,\dot{\phi}^{\circ,j},0,\dot{\theta}^{\circ,j},0,\dot{\psi}^{\circ,j}\right]^T$, $j=1,\ldots,M$ results in the following state space form for the jth operating point:

$$\begin{aligned} \dot{\mathbf{x}} &= \mathbf{A_j}\mathbf{x}+\mathbf{B_j}\mathbf{u}+\tilde{\mathbf{w}} \qquad (4)\\ \mathbf{x} &= \left[\delta\phi,\delta\dot{\phi},\delta\theta,\delta\dot{\theta},\delta\psi,\delta\dot{\psi}\right]^T \\ \mathbf{u} &= \left[\delta U_1,\delta U_2,\delta U_3,\delta U_4,\delta\Omega_r\right]^T \end{aligned}$$

where,

$$\mathbf{A_j} = \begin{bmatrix} 0 & 1 & 0 & 0 & 0 & 0 \\ 0 & 0 & 0 & \frac{I_{yy}-I_{zz}}{I_{xx}}\dot{\psi}^{\circ,j} & 0 & \frac{I_{yy}-I_{zz}}{I_{xx}}\dot{\theta}^{\circ,j} \\ 0 & 0 & 0 & 1 & 0 & 0 \\ 0 & \frac{I_{zz}-I_{xx}}{I_{yy}}\dot{\psi}^{\circ,j} & 0 & 0 & 0 & \frac{I_{yy}-I_{xx}}{I_{yy}}\dot{\phi}^{\circ,j} \\ 0 & 0 & 0 & 0 & 0 & 1 \\ 0 & \frac{I_{xx}-I_{yy}}{I_{zz}}\dot{\theta}^{\circ,j} & 0 & \frac{I_{xx}-I_{yy}}{I_{zz}}\dot{\phi}^{\circ,j} & 0 & 0 \end{bmatrix} \qquad (5)$$

$$\mathbf{B_j} = \begin{bmatrix} 0 & 0 & 0 & 0 & 0 \\ 0 & \frac{l_a}{I_{xx}} & 0 & 0 & \frac{J_r}{I_{xx}}\dot{\theta}^{\circ,j} \\ 0 & 0 & 0 & 0 & 0 \\ 0 & 0 & \frac{l_a}{I_{yy}} & 0 & \frac{J_r}{I_{yy}}\dot{\theta}^{\circ,j} \\ 0 & 0 & 0 & 0 & 0 \\ 0 & 0 & 0 & \frac{1}{I_{zz}} & 0 \end{bmatrix} \qquad (6)$$

and $\tilde{\mathbf{w}}$ is the additive external disturbance vector that affects the flight of the UqH.

The utilized parameters for the UqH attitude modeling in equations (5) and (6) are presented in Table I.

TABLE I
LINEARIZED UQH MODEL PARAMETERS

I_{xx}	Moment of Inertia of the UqH about the X axis
I_{yy}	Moment of Inertia of the UqH about the Y axis
I_{zz}	Moment of Inertia of the UqH about the Z axis
l_a	Arm length
J_p	Propeller inertia
J_r	Moment of inertia of the rotor about its axis of rotation

III. UQH CONSTRAINED FINITE TIME OPTIMAL CONTROL DESIGN

The constrained finite time optimal control scheme [13] is designed and experimentally applied for performing stabilization of the quadrotor around deviations from the nominal angles of operation (attitude control). The proposed control action affects only the angular rotations of the quadrotor, while a feed–forward controller is utilized in order to apply the necessary elevation thrust to the UqH. The overall control scheme is presented in Figure 2.

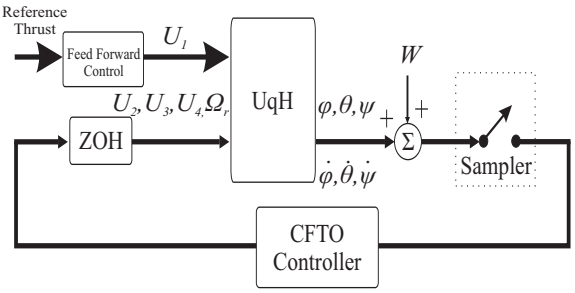

Fig. 2. UqH CFTO–control Scheme

For each operating point $\mathbf{x}^{\circ,\mathbf{j}}$, the UqH is assumed to operate within a regime specified by certain boundaries of its angular rates, or

$$\gamma^{\circ,j}-\Delta\gamma^j=\gamma_{\min}^{\circ,j}\le\delta\gamma\le\gamma^{\circ,j}+\Delta\gamma^j=\gamma_{\max}^{\circ,j},\ \gamma\in\left\{\dot{\phi},\dot{\theta},\dot{\psi}\right\}\ . \qquad (7)$$

In a similar manner, there are constraints related to the control inputs and the differential angles, denoted as

$$\delta U_i^{\min}\le\delta U_i\le\delta U_i^{\max},\ i\in\{1,2,3,4\} \qquad (8)$$

$$\delta\Omega_r^{\max}\le\delta\Omega_r\le\delta\Omega_r^{\max} \qquad (9)$$

$$-\Delta\gamma\le\delta\gamma\le\Delta\gamma,\ \gamma\in\{\phi,\theta,\psi\}\ . \qquad (10)$$

The systems' (4) discrete representations under the assumption of a T_s sampling period are:

$$\mathbf{x}_{k+1} = \mathbf{A}_j^* x(k)+\mathbf{B}_j^*+\mathbf{w}^*\ . \qquad (11)$$

For each discrete PWA-system in (11), 22–constraints from (7) thru (10) define its operating regime; these constraints

(guard functions in the CFTOC–terminology) can be written in a compact form as

$$\mathbf{H}_{i,j}\mathbf{x}+\mathbf{J}_{i,j}\mathbf{u}\leq\mathbf{D}_{i,j},\ i=1,\ldots,22,\quad j=1,\ldots,M. \qquad (12)$$

The CFTOC approach consists of computing the optimum control vector $\mathbf{U}_N=[u(0),\ldots,u(N-1)]$, with N the prediction horizon, which minimizes the following quadratic cost function:

$$J_N(x_0)=\min_{\mathbf{U}_N}\left\{\mathbf{x}(N)\mathbf{P}_N x(N)+\sum_{k=0}^{N-1}\mathbf{u}(k)^T\mathbf{R}\mathbf{u}(k)+\mathbf{x}(k)^T\mathbf{Q}\mathbf{x}(k)\right\} \quad (13)$$

subject to the PWA-system dynamics (11) and the state/input constraints (13). In the quadratic cost function in (13), $\mathbf{x}(0)$ is the currently available sample of the state vector, while $\mathbf{x}(k)$, with $k=0,\ldots,N-1$ are the predicted values of the state vector through equation (11) starting from $\mathbf{x}(0)$ and applying the input sequence $\mathbf{U}_N$. The positive definite and symmetric $\mathbf{Q}$, $\mathbf{R}$ and $\mathbf{P}_N$ weighting matrices apply the necessary penalty to the predicted states, control effort and the desired final state, respectively. The predicted final state $\mathbf{x}(N)$ belongs to a predefined set $\mathbf{x}(N)$ in $\mathscr{X}$ a choice typically dictated by stability and feasibility requirements.

It is well known [13–16], that the CFTOC optimizer is a continuous PWA–state feedback of the following form:

$$\mathbf{u}(k) \quad = \quad \mathbf{F}_l\mathbf{x}(k)+\mathbf{G}_l, \qquad if \qquad \mathbf{x}(k)\ \text{in}\ \mathbf{R}_l \quad (14)$$

defined over convex polyhedra $\mathbf{R}_l$, $l=1,\ldots,l^{\max}$ referred as "regions", which are also generated by the CFTO-algorithm. It should be noted that the number of polyhedra, $l^{\max}$ increases significantly with the number of operating points M, the dimension of the state vector (in the UqH-case, $\mathbf{x}\in\Re^6$), and the number of guard functions ($M\times 22$).

It should be noticed that the polyhedra and the feedback gains in (14) are computed in an off–line manner, and for the CFTOC's real–time implementation there is a search over the polyhedra–space and a subsequent mapping of the feedback gains from a lookup–table. The number of polyhedra, $l^{\max}$ is crucial for the real–time implementation of the CFTOC, since not only it affects the time needed for the search but also results in a large number of feedback gain transitions between regions [17, 18].

IV. EXPERIMENTAL STUDIES

For the experimental set–up the Draganfly Vti quadrotor helicopter has been utilized. The capabilities of this model have been increased in order to provide a computer–based feedback control of the UqH's attitude (Euler Angles and their derivatives). The radio control link between the computer and the UqH is achieved using a USB-6229 NI–board [19], connected with a FUTABA 6EXAP radio transmitter [20] operating in training mode. The feedback of the UqH's states is provided by the integration of the Xsens MTi-G [21] Attitude and Heading Reference System (AHRS) running a modification of the Extended Kalman Filter, with a wired data link between the AHRS unit and the computer. The wind gust velocities where measured using a rotary vane anemometer. The components of the experimental set–up are presented in Figure 3. In this figure the UqH is attached to a Heli-Safe$_{TM}$ flight test stand slightly modified in order to allow only attitude control. The wind–gust disturbances are created using an electric fan and an appropriately modified tunnel.

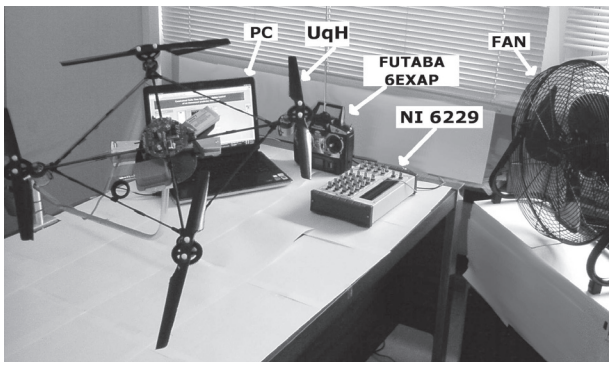

Fig. 3. UqH Attitude Control Experimental Set–Up

The parameters of the UqH considered were calculated using Computational Fluid Dynamics software and the technical data in [22] and have the values $I_{xx}=I_{yy}=5.0\cdot 10^{-3}$kg m^2, $I_{zz}=8.9\cdot 10^{-3}$kg m^2, $l_a=0.21$m, and $J_r=5.51\cdot 10^{-5}$kg m^2.

For the design and experimental application of the CFTO–control scheme various test cases were considered where the UqH model was approached by M–PWA systems with $M\in\{1,3,5\}$. In all these cases the sampling period was set to $T_s=0.5$sec, while for the case of the 3–PWA systems the utilized discrete time state space matrices in the simulation studies are:

$$\mathbf{A}_1^* = \begin{bmatrix} 1 & 0.5 & 0 & 0 & 0 & 0 \\ 0 & 1 & 0 & 0 & 0 & 0 \\ 0 & 0 & 1 & 0.5 & 0 & 0 \\ 0 & 0 & 0 & 1 & 0 & 0 \\ 0 & 0 & 0 & 0 & 1 & 0.5 \\ 0 & 0 & 0 & 0 & 0 & 1 \end{bmatrix},$$

$$\mathbf{B}_1^* = \begin{bmatrix} 0 & 5.3571 & 0 & 0 & 0 \\ 0 & 21.4286 & 0 & 0 & 0 \\ 0 & 0 & 5.3571 & 0 & 0 \\ 0 & 0 & 21.4286 & 0 & 0 \\ 0 & 0 & 0 & 14.2045 & 0 \\ 0 & 0 & 0 & 56.8182 & 0 \end{bmatrix}$$

for $-0.01<\dot{\theta},\dot{\phi},\dot{\psi}<0.01$,

$$\mathbf{A}_2^* = \begin{bmatrix} 1 & 0.5 & 0 & -0.0015 & 0 & -0.0015 \\ 0 & 1 & 0 & -0.0060 & 0 & -0.0060 \\ 0 & 0.0015 & 1 & 0.5 & 0 & 0.0015 \\ 0 & 0.0060 & 0 & 1 & 0 & 0.0060 \\ 0 & 0 & 0 & 0 & 1 & 0.5 \\ 0 & 0 & 0 & 0 & 0 & 1 \end{bmatrix},$$

$$\mathbf{B}_2^* = \begin{bmatrix} 0 & 5.3571 & -0.0107 & -0.0283 & 0 \\ 0 & 21.4284 & -0.0640 & -0.1699 & 0.0002 \\ 0 & 0.0107 & 5.3571 & 0.0282 & 0 \\ 0 & 0.0640 & 21.4284 & 0.1692 & 0.002 \\ 0 & 0 & 0 & 14.2045 & 0 \\ 0 & 0 & 0 & 56.8182 & 0 \end{bmatrix}$$

for $0.01 < \dot{\theta}, \dot{\phi}, \dot{\psi} < 0.05$, and

$$\mathbf{A}_3^* = \begin{bmatrix} 1 & 0.5 & 0 & 0.0015 & 0 & 0.0015 \\ 0 & 1 & 0 & 0.0060 & 0 & 0.0060 \\ 0 & -0.0015 & 1 & 0.5 & 0 & -0.0015 \\ 0 & -0.0060 & 0 & 1 & 0 & -0.0060 \\ 0 & 0 & 0 & 0 & 1 & 0.5 \\ 0 & 0 & 0 & 0 & 0 & 1 \end{bmatrix},$$

$$\mathbf{B}_3^* = \begin{bmatrix} 0 & 5.3571 & 0.0107 & 0.0282 & 0 \\ 0 & 21.4284 & 0.0640 & 0.1692 & -0.0002 \\ 0 & -0.0107 & 5.3571 & -0.0283 & 0 \\ 0 & -0.0640 & 21.4284 & -0.1699 & -0.0002 \\ 0 & 0 & 0 & 14.2045 & 0 \\ 0 & 0 & 0 & 56.8182 & 0 \end{bmatrix}$$

for $-0.05 < \dot{\theta}, \dot{\phi}, \dot{\psi} < -0.01$.

The tuning parameters of the CFTO–controller were $\mathbf{Q} = 10^6 \cdot \mathbf{I}_{6\times 6}$, $\mathbf{R} = 100 \cdot \mathbf{I}_{5\times 5}$, and the prediction horizon was set to $N = 4$, and $\mathbf{x}(N) = 0$ (regulation case).The initial state vector was $\mathbf{x}(0) = \mathbf{0}_{6\times 1}$. The constraints on the inputs have been computed based on the physical parameters of the system and specifically: a) the maximum angular velocity of the motor for maximum efficiency as provided from the manufacturer specifications [23], b) the thrust factor in hovering mode, computed as $b = 2.8 \cdot 10^{-5}$, and c) the drag factor in hovering computed as $d = 8 \cdot 10^{-7}$. Using these data, the following constraints on the inputs and the outputs were computed: $0 \le U_1 \le 11.23$, $|U_2| \le 5.61$, $|U_3| \le 5.61$, $|U_4| \le 0.16$. The constraints on the states were set:

$$\begin{bmatrix} -\pi/2 \\ -1 \\ -\pi/2 \\ -1 \\ -\pi \\ -1 \end{bmatrix} < \begin{bmatrix} \phi \\ \dot{\phi} \\ \theta \\ \dot{\theta} \\ \psi \\ \dot{\psi} \end{bmatrix} < \begin{bmatrix} \pi/2 \\ 1 \\ \pi/2 \\ 1 \\ \pi \\ 1 \end{bmatrix}.$$

The responses of the UqH's rotation angles (upper part), angular velocities (middle part), and the controller's effort (lower part) for a prediction horizon $N = 4$, with 3–PWA systems and without wind gusts are presented in Figure 4. The occurred steady state errors are obtained due to: a) calibration deviations of the IMU, and b) the non–linearities of the UqH's real model.

The responses for the roll (upper part), pitch (middle part) and yaw (lower part) for controllers computed based on different number of PWA systems (1, 3 and 5) are presented in Figure 5. The results obtained with the controller based on the 3–PWAs were slightly better (faster response, smaller steady state error) than the ones obtained with the other two controllers.

In the case where a 3–directional wind gust applied to the UqH (with a directional magnitude of x-1.38m/, y-3.86m/s, and z-1.67m/s) the responses of the rotational angles, for $M \in \{1,3,5\}$–PWA systems, are presented in Figure 6. In the beginning of the experiment, the UqH is close to its regulation point (until the 25th second); afterwards a steady wind gust is applied till the 125th second. From these results it is shown that as the number of PWA–systems increases in the controller design, the response of the UqH also improves. It should be noted that for the real–time implementation, when $M = 5$ the computer needed 0.49 seconds to compute the control effort, unlike the other cases in which the control effort could be generated in a significantly shorter period.

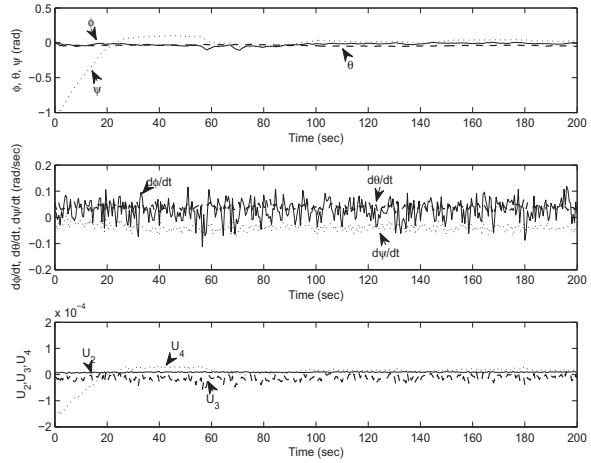

Fig. 4. UqH's Attitude Response and Control Effort ($M = 3$)

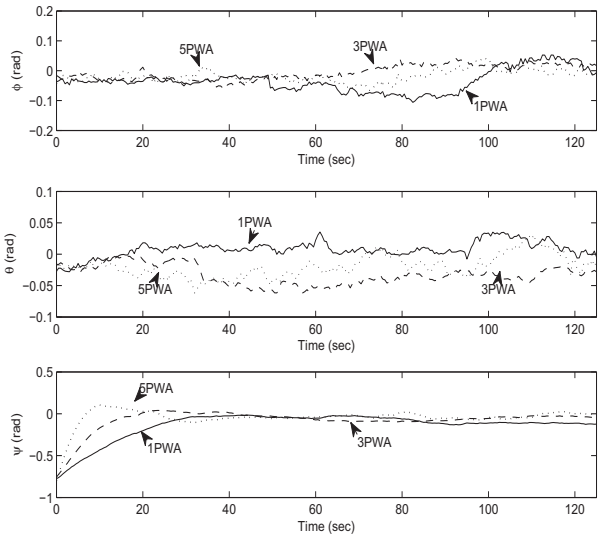

Fig. 5. UqH's RPY–angle responses in the absence of wind–gusts ($M \in \{1,3,5\}$)

There is a tradeoff between the complexity of the controller which stems from a large number of operating points and results in a smoother response, and the control effort needed to implement such an effective controller.

Rather than providing a large number of operating points in the CFTOC design process, a single ($M = 1$) point was selected resulting in a reduction of the sampling period due to the ease of implementation of the controller. In Figure 7 a comparison of the response for CFTO–controllers based on a single PWA and for sampling times equal to 0.5 and 0.1 seconds are presented, while the corresponding results for the case of presence of a three–directional wind–gusts are

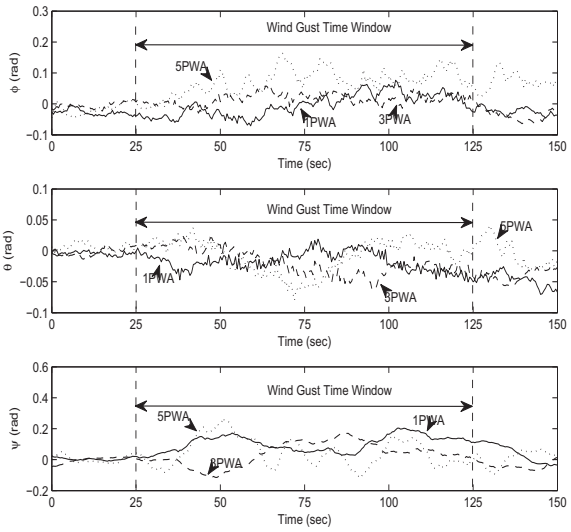

Fig. 6. UqH's RPY–angle responses subject to x(1.38 m/s), y(3.86m/s) and z(1.67m/s) directional wind gust ($M \in \{1,3,5\}$)

presented in Figure 8.

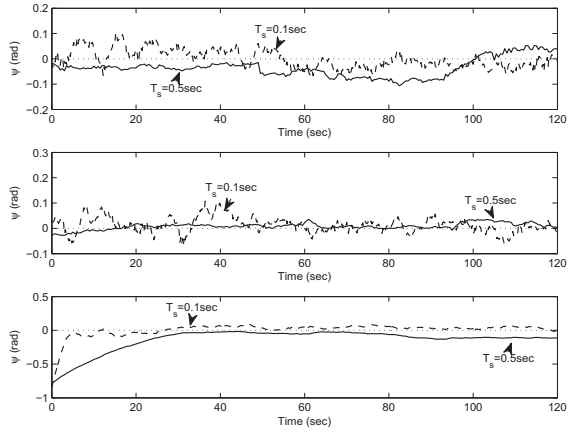

Fig. 7. UqH's RPY–angle responses in the absence of wind gust ($M = 1, T_s \in \{0.1,\ 0.5\}$ sec)

V. CONCLUSIONS

In this paper a CFTO–control scheme for the attitude control of an UqH subject to wind gusts has been presented. The resulting controller has been applied to an experimental set–up with a Draganfly Vti helicopter that has been modeled as a set of linear PWA systems. Multiple experimental results have been presented that prove the efficacy of the proposed controller both in nominal value regulation and wind gust disturbances attenuation.

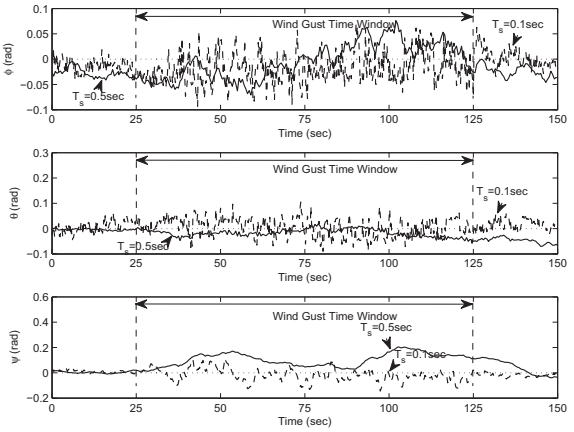

Fig. 8. UqH's RPY–angle responses subject to a x(1.38m/s), y(3.86m/s) and z(1.67m/s) directional wind–gust ($M = 1, T_s \in \{0.1,\ 0.5\}$ sec)

REFERENCES

[1] G. Hoffmann, D. G. Rajnarayan, S. L. Waslander, D. Dostal, J. S. Jang, and C. J. Tomlin, "The stanford testbed of autonomous rotorcraft for multi agent control (starmac)," in *23rd Digital Avionics Systems Conference*, vol. 2, 2004.

[2] S. Bouabdallah, P. Murrieri, and R. Siegwart, "Design and control of an indoor micro quadrotor," in *Robotics and Automation, IEEE International Conference on*, vol. 5, New Orleans, LA, April 2004, pp. 4393–4398.

[3] S. Bouabdallah, M. Becker, and R. Siegwart, "Autonomous miniature flying robots: coming soon! - research, development, and results," *Robotics & Automation Magazine, IEEE*, vol. 14, no. 3, pp. 88–98, 2007.

[4] L. Merino, F. Caballero, J. Martinez, and A. Ollero, "Cooperative fire detection using unmanned aerial vehicles," in *Robotics and Automation, IEEE International Conference on*, Barcelona, Spain, April 2005, pp. 1884–1889.

[5] N. Metni and T. Hamel, "A UAV for bridge inspection: Visual servoing control law with orientation limits," *Automation in Construction*, vol. 17, no. 1, pp. 3–10, November 2007.

[6] D. Murphy and J. Cycon, "Applications for mini VTOL UAV for law enforcement," in *Information and Training Technologies for law enforcement*, Boston, MA, November 1998.

[7] G. M. Hoffmann, H. Huang, S. L. Waslander, and C. J. Tomlin, "Quadrotor helicopter flight dynamics and control: Theory and experiment," in *Proc. of the American Institute of Aeronautics and Astronautics (AIAA) Guidance, Navigation, and Control Conference*, South Carolina, 2007.

[8] S. Bouabdallah, A. Noth, and R. Siegwart, "PID vs LQ control techniques applied to an indoor micro quadrotor," in *In Proceedings of the IEEE/RSJ International Conference on Intelligent Robots and Systems*, Sendai, Japan, 2004, pp. 2451–2456.

[9] A. Benallegue, A. Mokhtari, and L. Fridman, "Feedback linearization and high order sliding mode observer for a quadrotor UAV," in *International Workshop on Variable Structure Systems (VSS'06)*, Alghero, Sardinia, 2006, pp. 365–372.

[10] S. L. Waslander, G. M. Hoffmann, J. S. Jang, and C. J. Tomlin, "Multi-agent quadrotor testbed control design: Integral sliding mode vs. reinforcement learning," in *Proceedings of the IEEE/RSJ International Conference on Intelligent Robotics and Systems*, Alberta, Canada, 2005, pp. 468–473.

[11] S. Bouabdallah and R. Siegwart, "Full control of a quadrotor," in *Intelligent Robots and Systems, 2007. IROS 2007. IEEE/RSJ International Conference on*, 2007, pp. 153–158.

[12] S. Bouabdallah, "Design and control of quadrotors with application to autonomous flying," Ph.D. dissertation, STI School of Engineering, EPFL, Lausanee, 2007.

[13] M. Kvasnica, P. Grieder, M. Baotic, and M. Morari, *Multi-Parametric Toolbox (MPT)*, Automatic Control Laboratory, Swiss Federal Institute of Techonology (ETH), 2004.
[14] F. Borrelli and M. Baotic and A. Bemporad and M. Morari, "An Efficient Algorithm for Computing the State Feedback Optimal Control Law for Discrete Time Hybrid Systems," in *Proceedings of American Control Conference*, Denver, CO, June 2003, pp. 4717–4722.
[15] P. Grieder, F. Borelli, F. Torrisi, and M. Morari, "Computation of the constrained infinite time linear quadratic regulator," *Automatica*, vol. 40, no. 4, pp. 701–708, April 2004.
[16] G. Nikolakopoulos, L. Dritsas, A. Tzes, and J. Lygeros, "Adaptive constrained control of uncertain arma-systems based on set membership identification," in *Proceedings of the 14th IEEE Mediterranean Conference on Control and Automation (MED06)*, Ancona, Italy, June 2006.
[17] D. P. Bertsekas, *Dynamic Programming and Optimal Control*. Athena Scientific, 1995.
[18] R. W. Beard and T. W. McLain, "Multiple UAV cooperative search under collision avoidance and limited range communication constraints," in *42nd IEEE Conference on Decision and Control, 2003. Proceedings*, vol. 1, 2003.
[19] National Instruments, "NI USB-6229 BNC," *http://sine.ni.com/nips/cds/view/p/lang/en/nid/203866*.
[20] Futaba, "Futaba 6EXAP 6-channel PCM / PPM (FM) selectable Radio control system for aircraft," *http://manuals.hobbico.com/fut/6exas-manual.pdf*.
[21] Xsens, "Xsens MTi-G," *http://www.xsens.com/en/general/mti-g*.
[22] A. Tayebi and S. McGilvray, "Attitude stabilization of a VTOL quadrotor aircraft," *IEEE Transactions on Control Systems Technology*, vol. 14, no. 3, pp. 562–571, 2006.
[23] Mabuchi Motor, "Mabuchi rc-280sa," *http://www.mabuchi-motor.co.jp*.